Original

Zahn, M.; Akperov, M.; Rinke, A.; Feser, F.; Mokhov, I.I.:

Trends of Cyclone Characteristics in the Arctic and Their Patterns From Different Reanalysis Data

In: Journal of Geophysical Research : Atmospheres (2018) AGU

DOI: 10.1002/2017JD027439

AGU PUBLICATIONS

JGR

Journal of Geophysical Research: Atmospheres

RESEARCH ARTICLE
10.1002/2017JD027439

Key Points:
- Spatial patterns of Arctic cyclone trends are similar across different reanalysis products
- Frequency changes of Arctic cyclones are unrelated to changes in their intensity and size
- Deep Arctic cyclones and all Arctic cyclones take a reversed course across the year

Supporting Information:
- Supporting Information S1
- Figure S1
- Figure S2
- Figure S3
- Figure S4
- Figure S5
- Figure S6
- Figure S7
- Figure S8
- Figure S9
- Figure S10
- Figure S11

Correspondence to:
M. Akperov,
aseid@ifaran.ru

Citation:
Zahn, M., Akperov, M., Rinke, A., Feser, F., & Mokhov, I. I. (2018). Trends of cyclone characteristics in the Arctic and their patterns from different reanalysis data. *Journal of Geophysical Research: Atmospheres*, *123*, 2737–2751. https://doi.org/10.1002/2017JD027439

Received 11 JUL 2017
Accepted 15 DEC 2017
Accepted article online 1 MAR 2018
Published online 14 MAR 2018

Trends of Cyclone Characteristics in the Arctic and Their Patterns From Different Reanalysis Data

Matthias Zahn[1], Mirseid Akperov[2], Annette Rinke[3], Frauke Feser[1], and Igor I. Mokhov[2,4]

[1]Institute of Coastal Research, Helmholtz-Centre Geesthacht, Geesthacht, Germany, [2]A.M.Obukhov Institute of Atmospheric Physics, Russian Academy of Sciences, Moscow, Russia, [3]Alfred Wegener Institute, Helmholtz Centre for Polar and Marine Research, Potsdam, Germany, [4]Department of Physics, Lomonosov Moscow State University, Moscow, Russia

Abstract Cyclones in the Arctic are detected and tracked in four different reanalysis data sets from 1981 to 2010. In great detail the spatial and seasonal patterns of changes are scrutinized with regards to their frequencies, depths, and sizes. We find common spatial patterns for their occurrences, with centers of main activity over the seas in winter, and more activity over land and over the North Pole in summer. The deep cyclones are more frequent in winter, and the number of weak cyclones peaks in summer. Overall, we find a good agreement of our tracking results across the different reanalyses. Regarding the frequency changes, we find strong decreases in the Barents Sea and along the Russian coast toward the North Pole and increases over most of the central Arctic Ocean and toward the Pacific in winter. Areas of increasing and decreasing frequencies are of similar size in winter. In summer there is a longish region of increase from the Laptev Sea toward Greenland, over the Canadian archipelago, and over some smaller regions west of Novaya Zemlya and over the Russia. The larger part of the Arctic experiences a frequency decrease. All the summer changes are found statistically unrelated to the winter patterns. In addition, the frequency changes are found unrelated to changes in cyclone depth and size. There is generally good agreement across the different reanalyses in the spatial patterns of the trend sign. However, the magnitudes of changes in a particular region may strongly differ across the data.

1. Introduction

Cyclones are an important feature of the Arctic climate system. Carrying huge amounts of latent and sensible heat, they crucially affect the energy balance of the polar region. Accordingly, the two major storm tracks in the Northern Hemisphere are associated with the largest atmospheric energy input (Bengtsson et al., 2011, 2013) into the Arctic. Energy transports can be broken down into latent and sensible parts, and a thorough analysis of cyclones may provide insights into the role of different mechanisms driving moisture and heat transports to the Arctic as recently done by Dufour et al. (2016) or by Boisvert et al. (2016). In some extreme cases very intense cyclones can cause large anomalous warming over the Arctic (Graham et al., 2017; Kim, Hong, et al., 2017) and even lead to temperatures around 0 °C over the North Pole in winter (Moore, 2016), when normally mean temperatures around −30 °C prevail.

In addition to shifting energy, poleward cyclones also impact the sea ice concentration and melt (Boisvert et al., 2016; Simmonds & Keay, 2009), thus controlling atmospheric energy supply from the surface. Hence, any changes in cyclone activity directly impact the Arctic energy balance. Therefore, to understand Arctic amplification, regional trends of cyclone characteristics have to be quantified. For their robust assessment, it is important to know the (dis)agreement among different reanalyses.

One of the first studies to address changes of cyclone activity in four different reanalysis data sets globally finds that results are less variable in the northern hemisphere, while for the southern hemisphere, the results are more variable across the data (Hodges et al., 2003). Using ERA-40 and National Centers for Environmental Prediction (NCEP)/National Center for Atmospheric Research reanalysis data at different resolution, Hanson et al. (2004) compare cyclones over the North Atlantic and find differences in size and intensity in some Beaufort Scale categories. Using the same two reanalysis data, Trigo (2006) finds discrepancies in cyclone numbers, but agreement in their spatial distribution.

Simmonds et al. (2008) compare time series of cyclone occurrences over the Arctic and find disagreement in the trends across the reanalyses for the years 1979–2002.They conclude that trends can even differ in sign

across different reanalyses in some periods. Hence, any results for recent changes may be sensitive to the data applied in a respective study.

Over the last 10 years, several additional reanalysis-based data sets became available that often are at a much higher resolution. Hence, more recent studies apply more data sets to investigate cyclone characteristics.

That is, Tilinina et al. (2013) use five different reanalyses to analyze cyclone activity in the entire Northern Hemisphere over the 1979–1999 period. They find that the total number of cyclones strongly depends on the resolution and increases with increasing resolution of the reanalysis. They also present some spatial differences between the different data sets.

Also focusing on the entire Northern Hemisphere, Chang and Yau (2016) use five reanalysis data sets: NCEP, ERA-40, Japanese 55-year Reanalysis (JRA55), Twentieth Century Reanalysis, and ERA-20C. Compared to raw-insonde observation-based trends, changes in the NCEP data are found to be significantly larger or likely overestimated as they conclude. Those in ERA40 and JRA55 are closer but still biased.

Wang et al. (2016) perform a track-to-track comparison in nine reanalyses and find that track agreement larger than 30% (poorest) and up to 60% (best) in the Northern Hemisphere annually over the period 1979–2001, which is common in all data sets, and 10% and 40% in the southern.

Compared to all these global or hemisphere wide cyclone studies, there have been only very few studies focusing explicitly on the Arctic. A complete inventory is that of Zhang et al. (2004), who focus solely on the Arctic and create a cyclone activity index to describe their climatology and variability and investigate their spatial frequencies and intensities. Their study is based on NCEP/National Center for Atmospheric Research data and finds an increase in Arctic cyclone activity. Based on the same data, Sorteberg and Walsh (2008) provide characteristics of cyclones entering the Arctic and find an upward trend in the yearly averaged cyclone activity index (3% per decade), and Sepp and Jaagus (2011) show trends of total, deep, and shallow cyclone frequencies. In their analysis, the number of deep cyclones has increased over the past decades, while the number of shallow cyclones has decreased.

Most recently, Tilinina et al. (2014) have compared 11 (2000–2010) years of global high-resolution reanalyses (ERA-Interim, Modern-Era Retrospective analysis for Research and Applications [MERRA], and Climate Forecast System Reanalysis [CFSR]) to the Arctic System Re-Analysis (ASR) that has been produced exclusively for the Arctic. They report a considerably higher number of cyclones in ASR, which they explain with the higher resolution and more comprehensive data assimilation in ASR.

We here focus on the changing characteristics of cyclones in the Arctic in different reanalysis data sets (ERA-Interim, MERRA2, CFSR, and JRA55). We quantify the similarity in their seasonal cycle, in spatial patterns of their characteristics (frequency of occurrence, size, and depth), and in their trends over the last three decades. Thereby trends are not only investigated as accumulated numbers for certain subregions but also calculated for all areas at grid cell size. Thus, we gain the distribution of positive and negative changes and the spatial pattern of trends at very high spatial detail. Our main focus is to find any reasons explaining the differences in the studies comparing the results of cyclone tracking in reanalyses before.

2. Data

We used four commonly applied high-resolution reanalysis data sets, namely, ERA-Interim, National Aeronautics and Space Administration (NASA)-MERRA2, NCEP-CFSR, and JRA55 as listed in Table 1. From each data set we picked mean sea level pressure (MSLP) available four times per day (0:00,6:00,12:00, and 18:00) of the 30 year period 1981–2010. We chose this period, because it is widely covered by satellite observations, which enter the reanalysis products through their assimilation schemes. Prior to 1981, satellite coverage and thus the amount of data assimilated by the reanalyses was increasing and makes them prone to inhomogeneities. In addition, this is a period covered by all data set and 30 years are the standard period for climatological means.

We chose these four because they are the frequently used global data sets with the highest horizontal/vertical resolutions. In addition, they come from different institutions, from different continents. Hence, we assume that observations that enter the reanalyses through the data assimilation procedure and the physics in the individual models differ as much as possible from one data set to the other and the tracking results are as independent as possible.

Table 1
Data Sets Used, Their References, and Horizontal and Vertical Resolutions

Data set	Reference	Model horizontal resolution	Model vertical resolution
ERA-Interim	Dee et al. (2011)	0.75° (T255)	L60
NASA-MERRA2	Gelaro et al. (2017)	0.5° × 0.667°	L72
NCEP-CFSR	Saha et al. (2010)	0.5° (T384)	L64
JRA55	Ebita et al. (2011) Kobayashi et al. (2015)	0.55° (T319)	L60

Note. The number behind the T refers to the spectral wave at which the spectral models used to create the reanalyses are truncated. The number behind the L refers to the number of vertical levels in the reanalysis model.

The data are available globally, but we here use the data on the Arctic grid defined for the COordinated Regional climate Downscaling Experiment (CORDEX) project for the identification of cyclones. The Arctic CORDEX initiative (http://climate-cryosphere.org/activities/targeted/polar-cordex/arctic) is an international coordinated framework to produce an improved ensemble of regional climate change projections as the input for impact and adaptation studies aimed at a better understanding of the regional climate in the Arctic (Giorgi et al., 2009).

3. Method

We use a modified version of an algorithm developed to identify cyclones based on Bardin and Polonsky (2005) and Akperov et al. (2007). Details of the modifications consider the special conditions in the Arctic region and are described in Akperov et al. (2015). The algorithm is based on minima in the MSLP fields and has been applied in several other studies that investigate changes in cyclone activity in extratropical and high latitudes (Neu et al., 2013; Simmonds & Rudeva, 2014; Ulbrich et al., 2013).

More specifically, cyclone centers are identified as MSLP minima on the 6-hourly output data of each data set. If the MSLP at one grid point is lower than in the eight surrounding grid points, a candidate for a cyclone center is identified at this grid point. To locate its outermost closed isobar, we use a pressure step of 0.1 hPa from the previous grid point to identify the locations where the pressure no longer increases. These points then make up the outermost closed isobar. With this, we are able to calculate the depth (intensity) and the size (radius) of the cyclone. The coordinates of the grid node with minimal pressure are considered as the center of the cyclone. The size (radius) is determined as the average distance from the geometric center to the outermost closed isobar ($R = \frac{1}{n}\sum_{i=1}^{n} R_i$, where R_i is a radius from the center of the cyclone to its outermost, closed isobar, n is the number of nodes to the outermost closed isobar). The depth (intensity) is determined as the difference between the pressure in a cyclones geometric center and its outermost closed isobar. For connecting the centers to cyclone tracks, we connect two centers in consecutive time steps based on two criteria: a maximum search distance (600 km) and an allowable pressure difference (20 hPa). We did not use any restriction on cyclone lifetime and consider all tracks.

Note that there has been a discussion as to whether pressure or vorticity is more suitable for cyclone detection. That is, more than half of the cyclone identification methods presented in the IMILAST project (Neu et al., 2013) are pressure-based, while alternative approaches apply vorticity. Vorticity-based methods are more dependent on the spatial resolution and reproduce more small-scale cyclones than pressure-based methods. In the case of polar lows, Laffineur et al. (2014) cautioned to use vorticity for identification and tracking because vorticity maxima can also be associated with troughs. That MSLP methods work at least as well as vorticity-based ones also for larger cyclones has been shown in Colle et al. (2013). We thus decided to detect cyclones using MSLP. Prior to applying the identification and tracking, the reanalyses are interpolated onto the Arctic CORDEX grid (~50 km) using bilinear interpolation. The CORDEX grid is a rotated latitude-longitude grid at 0.5° × 0.5°. Along with this algorithm we record cyclone frequency, depth, and size. We applied the tracking to the CORDEX grid north of 60°N. For our analyses we use cyclone positions north of 65°N. This enables us to detect the size of the cyclones at the boundary of the area of investigation; that is, a cyclone location with its center at 65°N can extend as far south as 60°N.

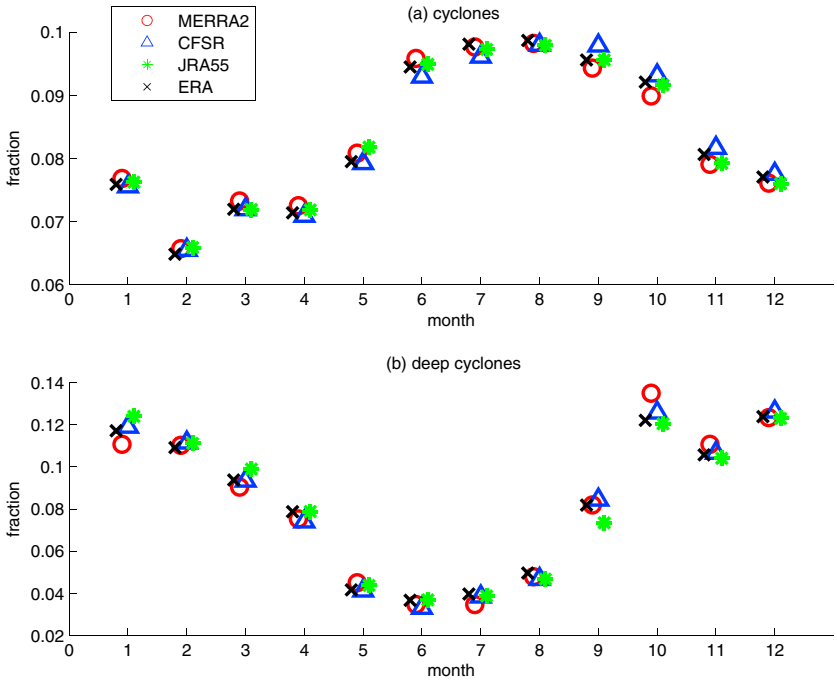

Figure 1. Annual cycle of cyclone frequency (fraction) for (a) all and (b) deep cyclones.

The cyclone frequency is defined as the total number of cyclone centers during the 30 year period divided by the overall number of days in each season.

The cyclone depth is determined as the difference between the minimum pressure in the cyclone center and the pressure of its outermost closed isobar. Cyclone depth is an important parameter because it is related to the influence a cyclone has through the net meridional transport and also here serves as a measure of cyclone total kinetic energy (Golitsyn et al., 2007; Simmonds & Keay, 2009). Those cyclones exceeding a depth lower than 95% of all cyclones are here termed deep cyclones. This 95th percentile corresponds to 19.6(±0.4) hPa in all the reanalyses.

All cyclones over areas of topography higher than 1,000 m, with a size less than 200 km or a depth less than 2 hPa, were considered too weak and have been excluded. We also want to minimize the influence of the reanalyses' different spatial resolution on the cyclone number. The higher resolved reanalyses may otherwise generate more cyclones at the smaller scales.

To map spatial patterns of cyclone frequency, we use a grid with circular cells of 2.5° latitude radius (or 250,000 km^2).

As an indicator for the robustness of any trends we calculated their statistical significance using the Student's *t* test.

When we split our results into summer and winter, we refer to the period December–January–February and June–July–August.

4. Arctic Cyclone Characteristics

4.1. Mean State

4.1.1. Annual Cycle

Figure 1 shows the annual cycle of all cyclones and of their most intense subset (deep cyclones) only. The overall numbers of Arctic cyclones peak in summer, when in July–September, the numbers are about 50% higher than in February–April. The annual course of deep cyclones, however, is the opposite. They are more than 3 times more frequent in winter than in summer. Their absolute numbers are in the order of 200 in summer, and 800 in winter, so we conclude that this is not a statistical artifact from too few cases.

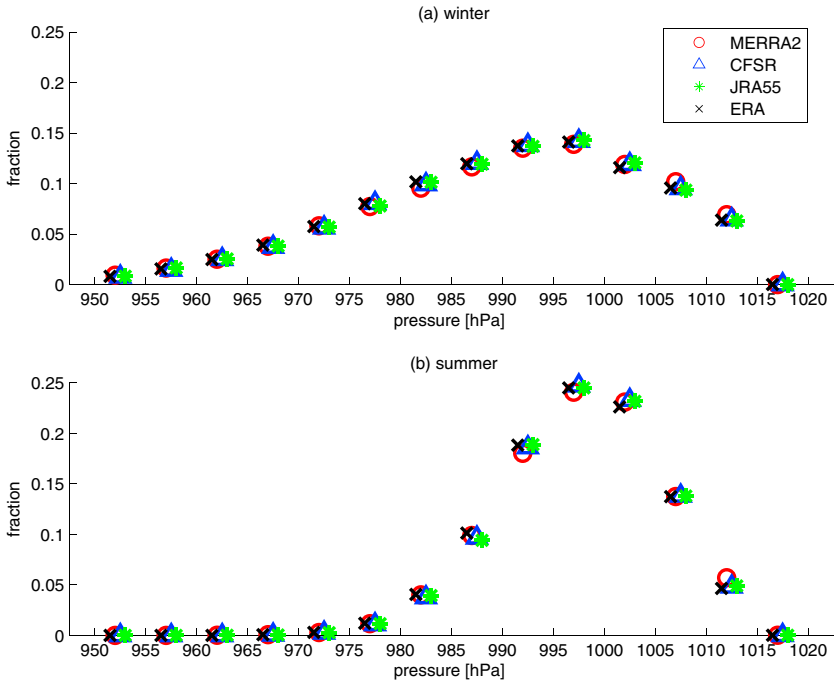

Figure 2. Distribution (fraction) of the minimum central pressure in the cyclones in (a) winter and (b) summer.

The winter peak of deep cyclones (Chang et al., 2012; Vavrus, 2013) and the summer peak of all Arctic cyclones (Zhang et al., 2004) have been shown separately in previous literature. The same can be derived from Table 1 in Sepp and Jaagus (2011) or Table 1 in Tilinina et al. (2014), but none of the previous studies stresses this opposite annual cycle of weak and intense cyclones; thus, we highlight this feature of Arctic cyclone occurrence.

The opposite annual cycle for all cyclones and for the subset of deep cyclones is shared by all four data sets, although the actual values may deviate slightly. In addition, the reanalyses also agree in the overall distribution of cyclone depth. They all denote the largest fraction for the weak cyclones that decreases toward the deeper ones (Figure S1).

If one assumes that the deep cyclones, which we define using the relative pressure difference, at the same time also have lower central pressures, the opposite annual cycle is also suggested in Figure 2. Their distribution is much narrower, and in favor of higher values in summer. In winter, more deep cyclones lift the distribution for the lower central pressures on the left. The distributions are again very similar across all reanalysis products.

We should mention that if we look at the cyclones' size distribution, MERRA2 has more smaller and less medium sized cyclones (Figure S2). Some bias in representing cyclones in MERRA, the predecessor of MERRA2, has been reported before, for example, by Tilinina et al. (2013) and Wang et al. (2016). The general picture, however, that there are by far more smaller cyclones in winter and that there is an opposite annual cycle of all and the deep cyclones are a common feature in all reanalyses.

4.1.2. Differences in Cyclone Characteristics Over Land and Ocean

Differences in cyclone characteristics across the reanalysis products have been reported in many previous studies (see section 1). Hence, the previous similarities are a bit surprising and we compare more thoroughly the different data. Figure 3 shows cyclone frequencies relative to the average result of all the four reanalyses as a reference, for all and for the deep cyclones, over land and over the ocean. Generally, more cyclones occur in summer, and the majority of cyclones develop over the oceans in both seasons (Table S1).

In winter overall numbers in ERA-Interim, CFSR and JRA55 are very similar and close to the average. Their absolute numbers are in the order of 10 per day. The largest difference is a 20% offset for all cyclones over

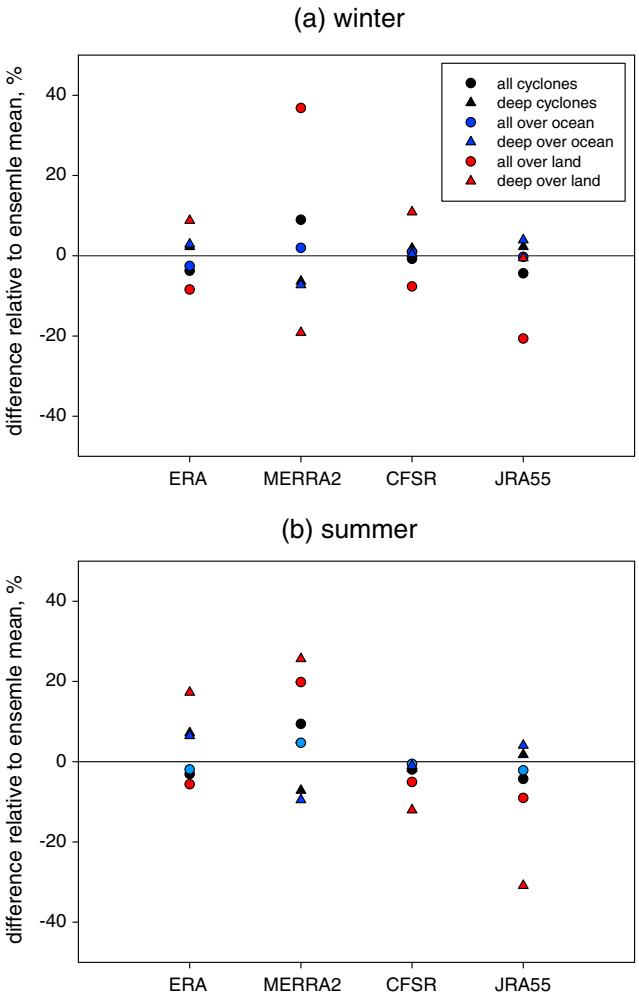

Figure 3. Relative cyclone frequency (black—over land and oceans, blue—over oceans, and red—over continents) when compared to the average of all reanalyses in (a) winter and (b) summer.

the continents in JRA55. MERRA2, however, generates an absolute number of 11 cyclones per day and has a bias of up to 40% more cyclones in total over the land, but about 20% less deep cyclones. The overall number in MERRA2 is about 10% higher for all cyclones, but about 8% lower for the deep ones. Both differences are below 5% in the other data.

Apparently, MERRA2 overestimates the number of weak, namely, non-deep, cyclones in the Arctic compared to the other reanalyses at the cost of the deep ones. This contrasts previous studies by, for example, Tilinina et al. (2013), who find the number of deep cyclones in MERRA too high compared to other reanalyses. However, our numbers may not be directly comparable, because Tilinina et al. (2013) use the older version of MERRA and apply restrictions to cyclone life cycle and travel distance, thereby filtering out many of the cyclones including deep ones. They also use an absolute threshold of 960 hPa for the core pressure to define deep cyclones, whereas we use a relative one dependent on the strength of the pressure gradient.

In summer overall absolute numbers are in the order of 13 per day, but MERRA2 stands out with 14.72 detected cyclones per day. Differences between the cyclone characteristics are generally larger, and, again, are largest over the continents. This is particularly the case for the subset of deep cyclones. The ability to generate and maintain these may be sensitive to the exact implementation of the different surface schemes in the reanalyses. In winter large parts of the Arctic land are snow-covered and energy exchanges between soil and the atmosphere are inhibited, or at least low. In summer, after the snow melted, these fluxes are important and may be treated differently in the models.

However, we should mention that there are fewer deep cyclones and the numbers may not be as significant as for the overall numbers. There are only 33/42 deep cyclones in total over the continents in JRA55/CFSR, and thus, large relative differences may not be too meaningful.

4.1.3. Spatial Characteristics

In the previous section, we have noted that apart from MERRA2, cyclone numbers are similar across the reanalyses in winter, but differences become larger over the land in summer. We here investigate in detail the spatial characteristics of cyclone frequency and their changes. In Figure 4, the spatial distributions of cyclone frequencies averaged across all four data products are presented, for summer and for winter. Their distributions from the individual reanalyses (Figures S3 and S4) are very similar. Hence, for brevity, we here just show their average. In winter we find three maxima of cyclone frequency, one in the Norwegian and Barents Sea, one in the Strait of Denmark between Iceland and Greenland, and one in the northern Baffin Bay. These are the well-known regions of Arctic cyclone occurrence in winter, which have already been identified in many previous studies (e.g., Raible et al., 2008).

In accordance with previous works (e.g., Zhang et al., 2004) cyclones show a stronger tendency to develop over land in summer. Then, the hot spot in the Barents Sea disappears, and some others emerge, over continental Siberia, Alaska, and over the central Arctic Ocean. The latter is also found in Simmonds et al. (2008) and is paid special attention to in Serreze and Barrett (2008), who conclude that cyclone systems generate outside and then travel into the central Arctic.

The methods in our study are applied to each reanalysis individually, and some of the results such as this average distribution are averaged for conciseness as in this case. The spatial patterns of the individual reanalyses confirm that there may be some differences in detail, especially in MERRA2, but generally the patterns agree well across all data sets.

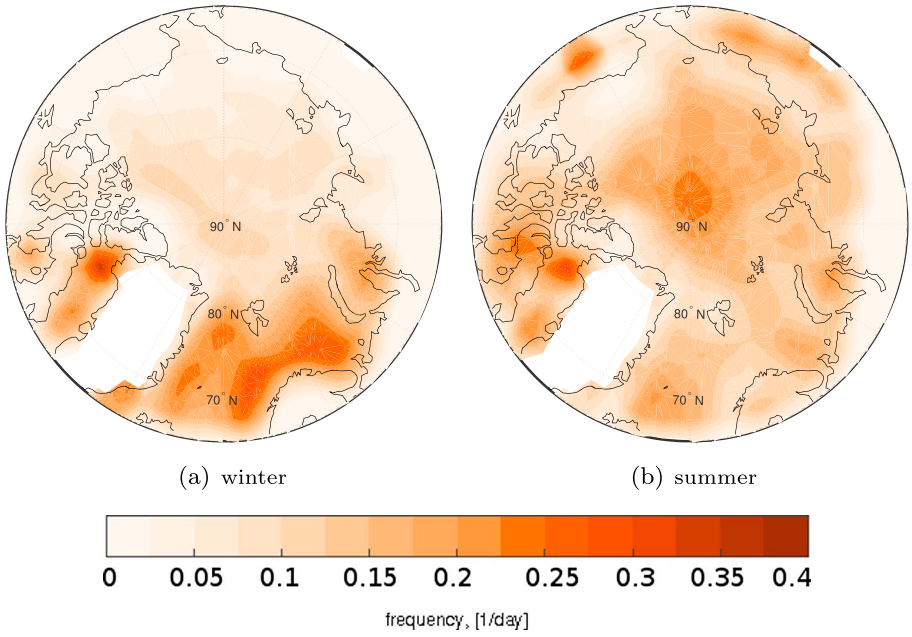

Figure 4. Spatial distribution of cyclone frequency for (a) winter and (b) summer averaged across all four reanalyses data.

4.2. Recent Changes

4.2.1. Spatial Patterns

To look at the development of cyclone characteristics over time, we show the recent spatial changes in frequency, depth, and size of cyclones in the Arctic over our investigation period 1981–2010, again separated into summer and winter (Figures 5–7).

The spatial patterns of the frequency trends share remarkable similarities across the reanalyses. In winter, there are two regions of significant cyclone frequency decline in all four data sets (Figure 5). One is in the Barents Sea, off the north-western Russian Arctic coast between the Kola Peninsula and Novaya Zemlya. The other one is in the Kara Sea, stretching along the North Russian coast between Novaya Zemlya and the Komsomolets Island up almost to the North Pole. There are also several smaller shared areas of decline, for example, off the coast of East Greenland, over the Canadian archipelago.

Shared significant increases in cyclone frequency are in the North Atlantic (northern part) around Spitsbergen, around an area from the North Pole stretching into the Beaufort Sea toward northern Canada, and in the northern Laptev and East Siberian Sea. Insignificant increases are calculated for the Norwegian Sea and Baffin Bay.

In summer (Figure 6) this pattern of increasing and declining cyclone frequency is unrelated to the winter pattern, and opposite at some places. In the Barents Sea region, parts of the Kara Sea and in the Taymyr Peninsula region, where the largest declines are found in winter, cyclone frequency increases in summer and the increase in cyclone frequency between the North Pole and the Beaufort Sea in winter turns into a strong decline in summer.

The remarkable similarity of the trend patterns across the reanalyses generally prevails in summer and only the spatial extensions change slightly. All data agree by and large in decreasing cyclone frequencies over most parts of the North Atlantic, in the Baffin Bay, and over eastern Siberia. Regions of increasing occurrence of cyclones are generally found over the Laptev Sea all the way north to the North Pole and over the Canadian Arctic archipelago.

Only two smaller disagreements emerge. One is in the southern Baffin Bay at the coast of Greenland, where MERRA2 is the only data set to show a regionally restricted but strong increase of cyclones. Another one is found over Alaska/North-West Canada, where ERA-Interim and JRA55 have positive, MERRA2 negative, and CFSR virtually no trends.

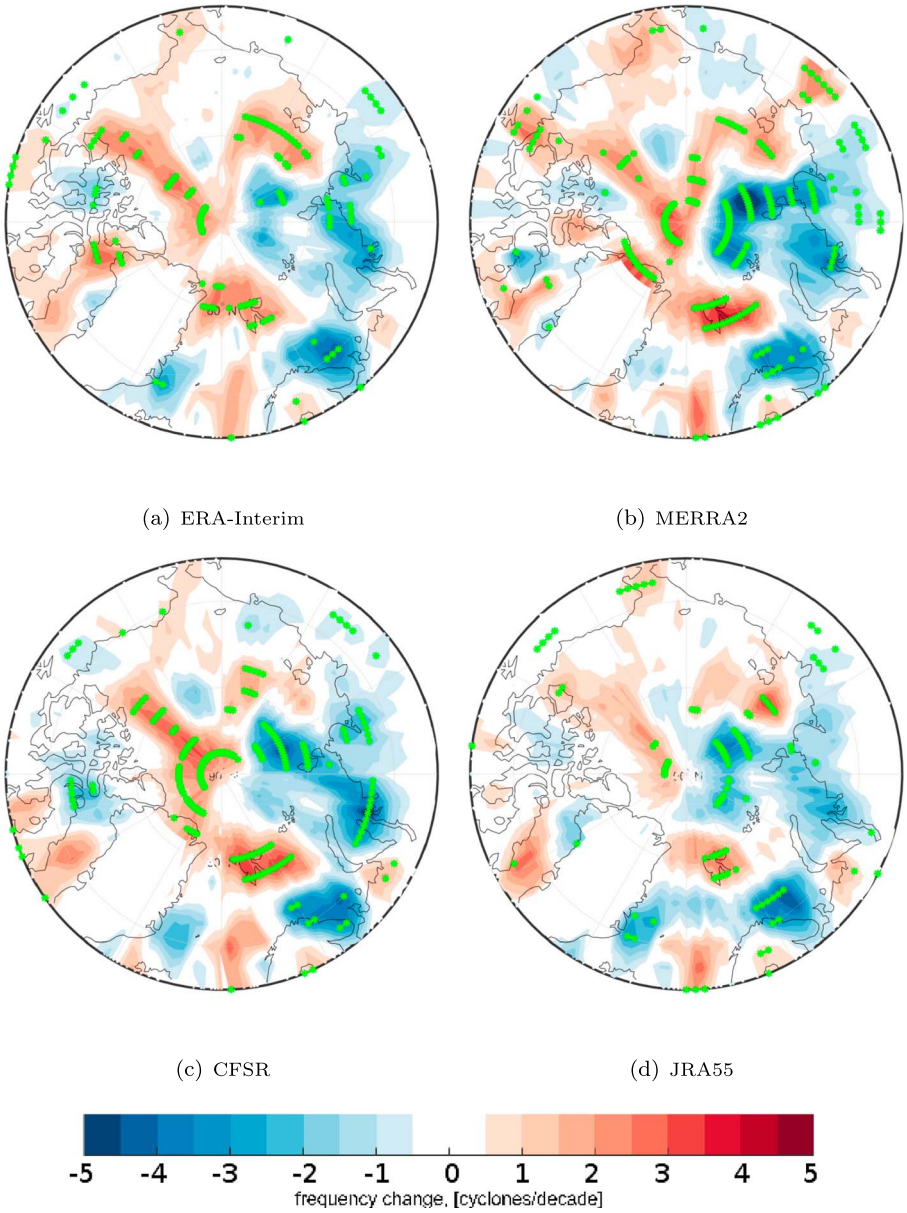

Figure 5. 30-year trends (1981–2010) of winter cyclone frequency in each grid box. The green asterisks show statistical significance at the 90% level.

The similarities between the trend patterns in the reanalyses are quantified with spatial pattern correlation coefficients as listed in Table 2. They confirm the remarkable agreement across the data. All coefficients are above 0.7, and many of them even above 0.8.

Although the patterns of change are quite similar, locally, the strengths of changes may differ substantially. For example, in MERRA2, the summer trend is ≈ -2 cyclones/decade and statistically significant along the Norwegian coast, but only half as strong (≈ -1.0 cyclones/decade) and not significant in ERA-Interim. However, the magnitude of a trend in a particular grid-box may be very sensitive to the few observations it is determined from.

In the same way, we compared the changes in cyclone depth and size from the different data. Again, we found a remarkable agreement across the data, and spatial pattern correlation coefficients in the order of 0.5 (Tables 3 and 4), though they are a bit lower than the similarities in frequencies.

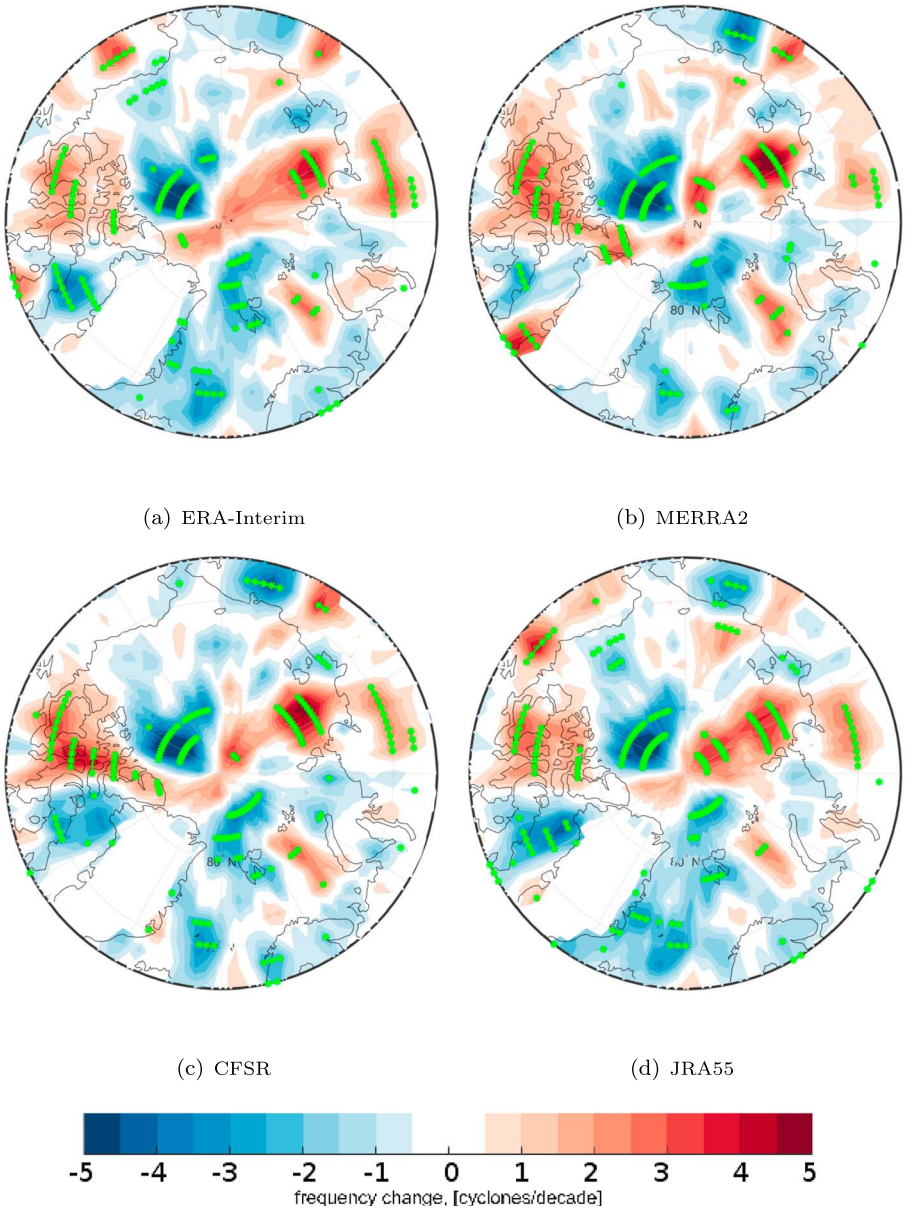

Figure 6. 30-year trends (1981–2010) of summer cyclone frequency in each grid box. The green asterisks show statistical significance at the 90% level.

Due to the similarity of the changes in space, we only show the average changes of depth and size in summer and winter (Figure 7). The results for each re-analysis individually can be found in the supporting information (Figures S5, S6, S7 and S8). Depth and size changes in winter are very patchy, with most of the region between the North Pole and the Pacific experiencing positive changes. Positive trends are also found in the Atlantic, over Svalbard and in the Barents/Kara Seas. Recall, that positive trends for depth mean that the cyclones become deeper. There is only one exception where the four data sets do not agree: ERA-Interim shows an extended region of cyclone size decrease over the northern Canadian archipelago, where all the three others have a positive trend (not shown).

In summer, most parts of the Arctic see a decline in cyclone depth and size, and increases are found mainly over land. Over the sea, only the Barents Sea shows a significant increase in depth and size.

Overall, there is a strong coincidence of cyclone depth and size increase/decrease. Both variables spatially change in a very similar way, and cyclones become either deeper and larger or less deep and smaller at

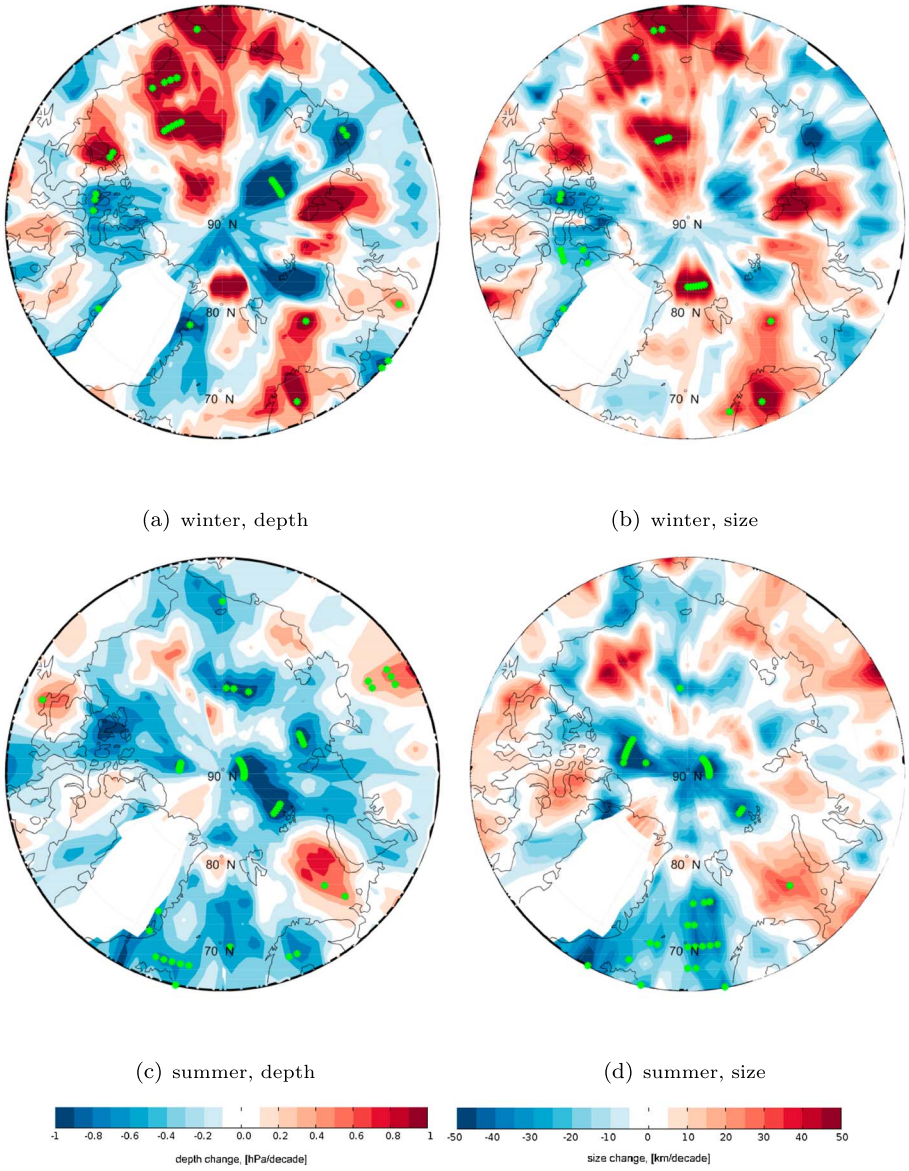

Figure 7. 30-year trends (1981–2010) for (a and c) depth and (b and d) size in winter (a and b) and summer (c and d), averaged across all reanalyses. The green asterisks show statistical significance at the 90% level.

Table 2
Spatial Correlation Coefficients Between the Trends of Cyclone Frequency in the Different Data

	ERA	MERRA2	CFSR	JRA55
ERA	\	***0.78***	***0.86***	***0.90***
MERRA2	**0.79**	\	***0.87***	***0.77***
CFSR	**0.82**	**0.81**	\	***0.84***
JRA55	**0.78**	**0.68**	**0.72**	\

Note. Winter: lower left triangle, summer: upper right triangle (bold-italics). All correlations are significant at the 99% level and are in bold.

the same time. This means that regions that have experienced more/less deep cyclones over the past also have seen larger/smaller ones. Intensification is accompanied by an enlargement of cyclones, and weakening by a reduction of their size.

4.2.2. Overall Trends

Here we summarize the more complex trend patterns of the previous section in one figure and present their aggregated changes in frequency, depth, and size over our investigation period in one number per season and data set in Figure 8.

The results confirm that the data agree in the changes of recent cyclone characteristics. This is particularly evident for the size and depth trends, which are either all positive (winter) or all negative (summer) over the

Table 3
Spatial Correlation Coefficients Between the Trends of Cyclone Depth in the Different Data

	ERA	MERRA2	CFSR	JRA55
ERA	\	***0.68***	***0.67***	***0.81***
MERRA2	**0.58**	\	***0.70***	***0.65***
CFSR	**0.68**	**0.61**	\	***0.59***
JRA55	**0.64**	**0.54**	**0.60**	\

Note. Winter: lower left triangle, summer: upper right triangle (bold-italics). All correlations are significant at the 99% level and are in bold.

entire regions, although the spatial correlations across the data were smaller than for the frequencies.

For the cyclone frequency changes, the picture is not so clear. If all cyclones are used, ERA-Interim and MERRA2 show an overall increase in winter, while CSFR shows a small and JRA55 a slightly larger overall decrease. The reason for JRA55 differing could be a less intense increase over the Laptev Sea, and a stronger decrease over the Baffin Bay, that affects the aggregated number of the overall trend. This highlights the necessity to look at the overall picture of the pattern of changes, because a single number may be very sensitive to deviations in individual subregions and thus not representative for the overall conditions.

The situation is a bit more uniform for deep cyclones. In winter they become more frequent, and only JRA55 shows a slightly negative change. In summer the signal of change is a decrease uniformly across the data. Note that the absolute numbers of deep cyclones in summer are only in the order of 40, and hence, very sensitive to few cases and even four cyclones less per summer can lead to percentage differences of 10%.

Over the ocean, negative trends of cyclone frequency, depth, and size are found in summer, while increases are usually found in winter (Figure S9). Over land, the situation is more complex and not even consistent across the reanalyses for all characteristics and seasons. However, cyclone numbers over land are lower and thus may be statistically less meaningful.

5. Discussion

5.1. Cyclone Matching Analysis

As previous papers have found that the exact numbers of Arctic cyclones in reanalyses can be very sensitive to the data, we began our work with the expectation to find relatively large differences for the cyclone characteristics.

In contrast, we have found strong similarities of detected cyclones across the reanalyses over the Arctic. This is, to some extent, surprising, because the Arctic regions are relatively sparse in meteorological observations. Thus, reanalysis data are less constrained in these areas and would here be expected to deviate from each other more than in other regions.

To validate the similarities across the data, we perform a cyclone matching analysis; that is, we determine if cyclones in one database have counterparts in the other data sets. For each detected location in the one reanalysis data set, we looked in the three other whether there is a location within a distance closer than 250 km at the same time step. Figure 9 shows for how many percent of the locations that a counterpart is found in only one, two, or in all three other data sets.

About 60% of the locations have a counterpart in all three other data, and only about 10% are detections without any equivalent. In other words, there is a 60% total agreement in the locations, and only 10% are clearly unmatched, either because of some algorithm shortcomings or because of some data problems.

If we merge the locations to their tracks and assume a track agreement if at least half of a track's positions have matching locations, the numbers even increase to about 70%. Only MERRA2 decreases to about 50%, which may be due to about 15% more detected locations than in the other data. These numbers are higher than in any other similar studies.

For example, Wang et al. (2016) in their track-to-track comparison find for the high-resolution reanalyses (ERA-Interim, MERRA, CFSR and JRA55) an agreement in the order of 40%. They use a region stretching as far south as 20°N, where actually more observations are available and similarities should be larger. Hodges et al. (2003) find track matching larger than 60% and up to 81% in the entire Northern Hemisphere, but they filter out all cyclones of less than two-day lifetime. Hence, they only use the most distinct cyclones that are more likely to be included in all data sets.

Table 4
Spatial Correlation Coefficients Between the Trends of Cyclone Size in the Different Data

	ERA	MERRA2	CFSR	JRA55
ERA	\	***0.63***	***0.56***	***0.75***
MERRA2	**0.52**	\	***0.52***	***0.63***
CFSR	**0.54**	**0.48**	\	***0.55***
JRA55	**0.46**	0.41	**0.49**	\

Note. Winter: lower left triangle, summer: upper right triangle (bold-italics). All correlations significant at the 99% level and are in bold (only one is not).

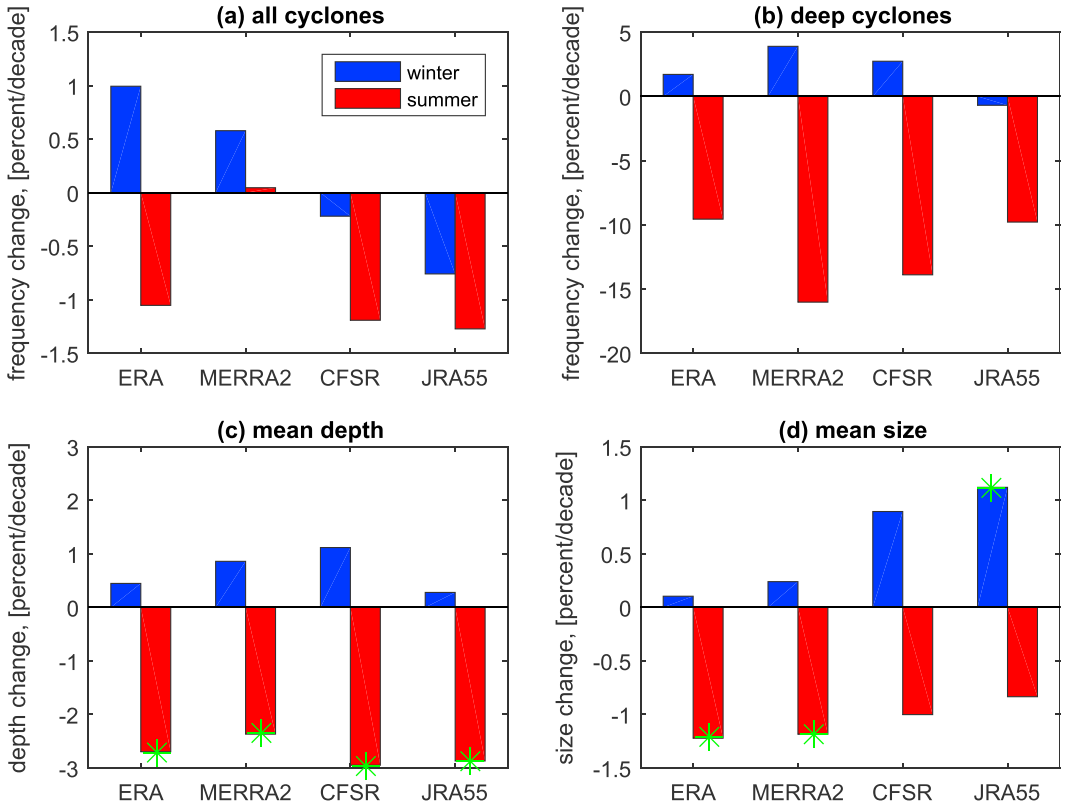

Figure 8. 30-year trends (1981–2010) of cyclone frequency (per decade) for (a) all cyclones, (b) deep cyclones, (c) cyclone mean depth, and (d) size for winter (blue) and summer (red), averaged over the Arctic. The green asterisks denote statistical significance at the 90% level.

If we perform the matching analysis for the weak locations (depth $\leq$ 4 hPa) only (Figure S10), the agreement in all data sets is in the order of 20%, and those with no matches at all also in the order of 20%. Only MERRA2 fares worse for the weak cyclones. If we consider that many of the weak cyclones may be small and just at the edge of what can be resolved in the reanalyses, a 20% agreement is still high and a complete disagreement of 20% of the locations is low. If we just use strong locations (depth $\geq$ 11 hPa), the numbers of total overlap increase to about 70%, and those without any decrease to only about 5% (Figure S11). To highlight that these values support the agreement across the reanalyses, we performed a random experiment in which we substitute the locations of the cyclones with random locations. These locations are equally distributed in space in our investigation area, but the same times as in the original data were used. There is practically no occurrence ($<$0.01%) of an overall agreement, and the number of no matches at all is around 90%. Even the chance for an overlap in only two data sets is in the order of only 3%. We conclude that there is indeed a strong agreement in cyclones and their statistical properties across the reanalyses.

The number of observations used in the assimilation process increases with time. Hence, there may be a time dependence of the similarities. The inspection of the evolution of the yearly matches shows a weak increase per year (not shown). This could point to more data assimilated over time leading to a higher similarity across the data. However, the trend was not found significant.

5.2. Differences Across the Reanalyses Over Land

Here we find the differences in Arctic cyclone characteristics relatively small, and differences are only large over land in summer, when deep cyclones are rare and relative differences are more sensitive to single cases. The increase in cyclone numbers from one reanalysis product to the other may be related with data resolution, which has been already noted in Blender and Schubert (2000). In this case, however, they influence both oceanic and continental cyclones. Tilinina et al. (2013) noted the impact of moderate and shallow cyclones on the total count of cyclones in the reanalyses, wherein the largest across data set spread in cyclone counts was

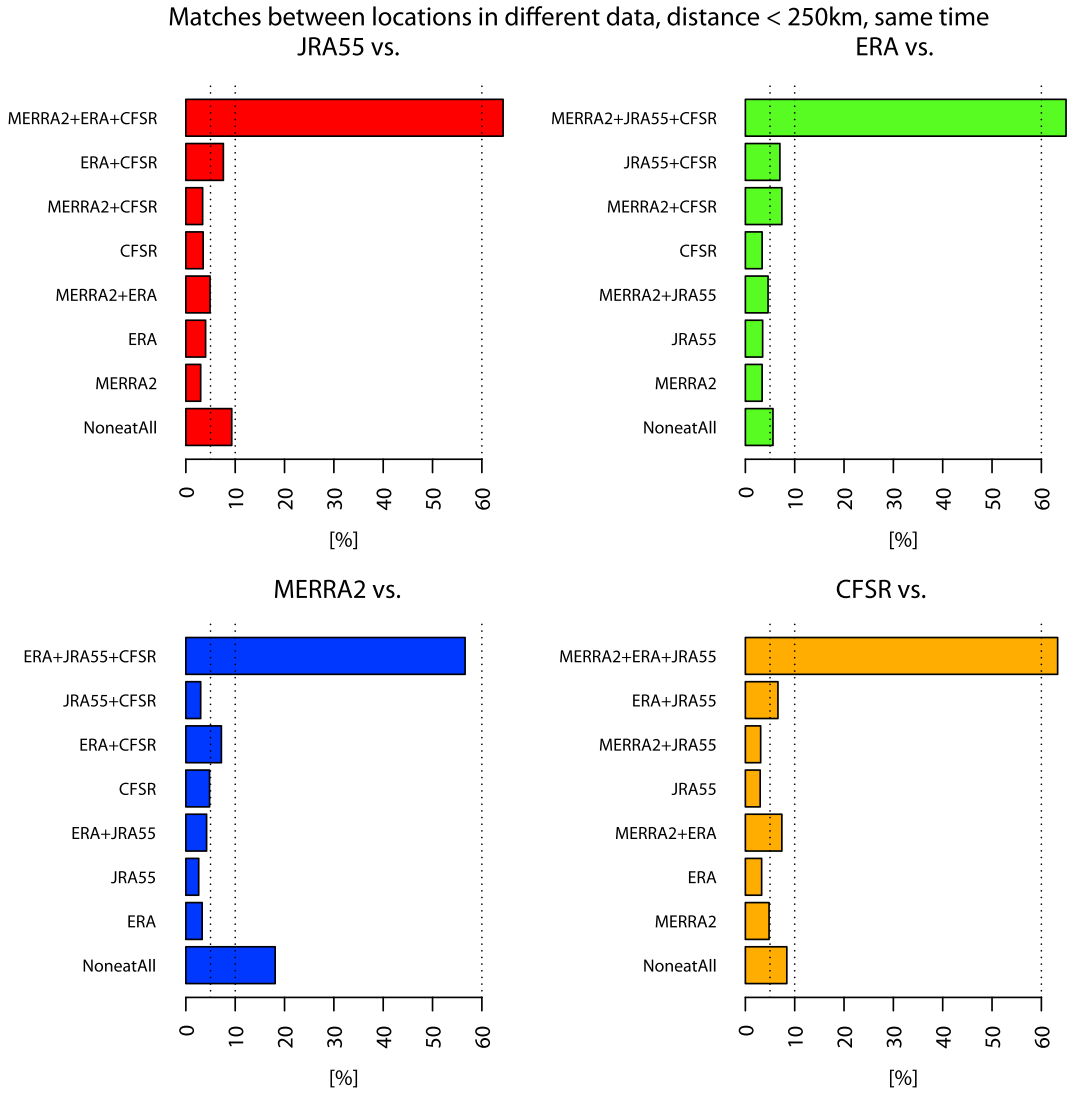

Figure 9. Percentage of matching locations relative to the respective reference data set. For each location in a reference reanalysis, it is checked whether there is at least one location in any of the other reanalyses closer than 250 km at the same time step. Note that the numbers are not cumulative; that is, if for a location in JRA55 a matching location is found in ERA-interim and MERRA2, this location is not considered for the ERA-Interim only bar.

also found to occur over the continents. Tilinina et al. (2014) also noted that the Arctic system reanalysis shows a considerably higher number of cyclones over the Arctic with the largest differences over the high-latitude continental areas relative to ERA-Interim. We argue that the larger differences in summer are at least partly due to the fact that energy exchanges between soil and atmosphere play a significant role in summer, while they are inhibited by snow cover in winter (Kim, Ray, & Choi, 2017). These fluxes can affect the baroclinicity and thus cyclone development and atmospheric circulation due to the dynamical impact of the atmosphere-land coupling (Matthes et al., 2012, 2017).

The surface sensible and latent turbulent heat fluxes are sensitive to the surface model, the surface radiative fluxes, and the atmospheric state. Recently, it has been shown that they depend strongly on the model physics and data assimilation procedures and the greatest variability of the surface fluxes between the reanalyses is over land (Bourassa et al., 2013; Lindsay et al., 2014).

We hypothesize that the uncertainties introduced through the variability of the surface fluxes and model physics over land are more important than the stronger constraints due to more data available for assimilation over land.

6. Summary

We apply cyclone tracking to the Arctic atmosphere in four high-resolution reanalysis data sets and investigate spatial trends in their characteristics. We find a realistic representation of the mean state, and we show that there is an opposite annual cycle in the frequency of deep and all cyclones. This is not a new finding, but as a straight message, this has not been emphasized elsewhere.

We further identify regions of increasing and decreasing cyclone frequencies over the investigation period 1981–2010 by calculating the trends in each model grid box. The actual magnitudes of trends can differ in strength, but patterns across the reanalyses are in good agreement across the data sets. This is in opposition to many previous studies that found sometimes large deviations. We suggest a reason may be that we do not just compare trend curves in defined areas but look at similarities in spatial patterns of trends. These are not very sensitive to differences in numbers or to differences in a particular subregion. In such subregions different magnitudes of changes or a small offset of the pattern in one data set may result in weaker relations, especially in regions with a strong gradient from positive to negative changes. We also note an agreement in size and depth, and in their changes.

In addition, we can infer that the patterns of changes in winter and summer are unrelated for all variables. The spatial correlations of cyclone frequency, depth, or size trends between summer and winter are close to zero, respectively (not shown). The same holds for the relation between frequency changes and size/depth changes in either winter or summer, for which we calculated spatial correlations in the order of 0.1 (not shown).

Acknowledgments

The work was supported through the Cluster of Excellence "CliSAP" (EXC177), University of Hamburg, funded through the German Research Foundation (DFG). It is a contribution to the Helmholtz Climate Initiative REKLIM (Regional Climate Change), a joint research project of the Helmholtz Association of German research centers (HGF). Annette Rinke has been supported by the SFB/TR172 Arctic Amplification: Climate Relevant Atmospheric and Surface Processes, and Feedback Mechanisms $(AC)^3$ funded through the German Research Foundation (DFG). Igor Mokhov has been supported by the Russian Science Foundation under gran14-17-00806 with the use of results obtained under the frame RAS programs. Mirseid Akperov has been supported by the Russian Science Foundation under grant14-17-00647. Mirseid Akperov, Igor Mokhov and Annette Rinke acknowledge the support by the project "Quantifying Rapid Climate Change in the Arctic: regional feedbacks and large-scale impacts (QUARCCS)" funded by the Russian and German Ministries of Research and Education. We acknowledge the Japan Meteorological Agency (JMA) for providing JRA55 (Ebita et al., 2011; Kobayashi et al., 2015), the European Centre for Medium-Range Weather Forecasts (ECMWF) for providing ERA-Interim (Dee et al., 2011), the National Centers for Environmental Prediction (NCEP) for providing NCEP-CFSR (Saha et al., 2010), and the NASA Goddard Earth Sciences (GES) Data and Information Services Center (DISC) for providing MERRA-2 (Gelaro et al., 2017). Their 6-hourly data were downloaded from https://reanalyses.org/atmosphere/overview-current-atmospheric-reanalyses.

References

Akperov, M. G., Bardin, M. Y., Volodin, E. M., Golitsyn, G. S., & Mokhov, I. I. (2007). Probability distributions for cyclones and anticyclones from the NCEP/NCAR reanalysis data and the INM RAS climate model. *Izvestiya Atmospheric and Oceanic Physics*, *43*(6), 705–712. https://doi.org/10.1134/S0001433807060047

Akperov, M., Mokhov, I., Rinke, A., Dethloff, K., & Matthes, H. (2015). Cyclones and their possible changes in the Arctic by the end of the twenty first century from regional climate model simulations. *Theoretical and Applied Climatology*, *122*(1–2), 85–96. https://doi.org/10.1007/s00704-014-1272-2

Bardin, M. Y., & Polonsky, A. B. (2005). North Atlantic oscillation and synoptic variability in the European-Atlantic region in winter. *Izvestiya Atmospheric and Oceanic Physics*, *41*(3), 127–136.

Bengtsson, L., Hodges, K., Koumoutsaris, S., Zahn, M., & Keenlyside, N. (2011). On the atmospheric water cycle of the polar regions. *Tellus A*, *63*(5), 907–920. https://doi.org/10.1111/j.1600-0870.2011.00534.x

Bengtsson, L., Hodges, K., Koumoutsaris, S., Zahn, M., & Berrisford, P. (2013). The changing energy balance of the polar regions in a warmer climate. *Journal of Climate*, *26*(10), 3112–3129. https://doi.org/10.1175/JCLI-D-12-00233.1

Blender, R., & Schubert, M. (2000). Cyclone tracking in different spatial and temporal resolutions. *Monthly Weather Review*, *128*(2), 377–384. https://doi.org/10.1175/1520-0493(2000)128%3C0377:CTIDSA%3E2.0.CO;2

Boisvert, L. N., Petty, A. A., & Stroeve, J. C. (2016). The Impact of the Extreme Winter 2015/16 Arctic Cyclone on the Barents–Kara Seas. *Monthly Weather Review*, *144*(11), 4279–4287. https://doi.org/10.1175/MWR-D-16-0234.1

Bourassa, M. A., Gille, S. T., Bitz, C., Carlson, D., Cerovecki, I., Clayson, C. A., et al. (2013). High-latitude ocean and sea ice surface fluxes: Challenges for climate research. *Bulletin of the American Meteorological Society*, *94*(3), 403–423. https://doi.org/10.1175/BAMS-D-11-00244.1

Chang, E. K. M., & Yau, A. M. W. (2016). Northern Hemisphere winter storm track trends since 1959 derived from multiple reanalysis datasets. *Climate Dynamics*, *47*(5-6), 1435–1454. https://doi.org/10.1007/s00382-015-2911-8

Chang, E. K. M., Guo, Y., & Xia, X. (2012). CMIP5 multimodel ensemble projection of storm track change under global warming. *Journal of Geophysical Research*, *117*, D23118. https://doi.org/10.1029/2012JD018578

Colle, B., Zhang, Z., Lombardo, K., Liu, P., Chang, E., & Zhang, M. (2013). Historical evaluation and future prediction in eastern North America and western Atlantic extratropical cyclones in the CMIP5 models during the cool season. *Journal of Climate*, *26*(18), 6882–6903. https://doi.org/10.1175/JCLI-D-12-00498.1

Dee, D. P., Uppala, S. M., Simmons, A. J., Berrisford, P., Poli, P., Kobayashi, S., et al. (2011). The ERA-Interim reanalysis: Configuration and performance of the data assimilation system. *Quarterly Journal of the Royal Meteorological Society*, *137*(656), 553–597. https://doi.org/10.1002/qj.828

Dufour, A., Zolina, O., & Gulev, S. K. (2016). Atmospheric moisture transport to the Arctic: Assessment of reanalyses and analysis of transport components. *Journal of Climate*, *29*(14), 5061–5081. https://doi.org/10.1175/JCLI-D-15-0559.1

Ebita, A., Kobayashi, S., Ota, Y., Moriya, M., Kumabe, R., Onogi, K., et al. (2011). The Japanese 55-year Reanalysis "JRA-55": An interim report. *SOLA*, *7*, 149–152. https://doi.org/10.2151/sola.2011-038

Gelaro, R., McCarty, W., Suárez, M. J., Todling, R., Molod, A., Takacs, L., et al. (2017). The Modern-Era Retrospective Analysis for Research and Applications, Version 2 (MERRA-2). *Journal of Climate*, *30*(14), 5419–5454. https://doi.org/10.1175/JCLI-D-16-0758.1

Giorgi, F., Jones, C., & Asrar, G. R. (2009). Addressing climate information needs at the regional level: The CORDEX framework. *WMO Bulletin*, *58*(3), 175–183.

Golitsyn, G. S., Mokhov, I. I., Akperov, M. G., & Bardin, M. Y. (2007). Distribution functions of probabilities of cyclones and anticyclones from 1952 to 2000: An instrument for the determination of global climate variations. *Doklady Earth Sciences*, *413*(1), 324–326. https://doi.org/10.1134/S1028334X07020432

Graham, R. M., Rinke, A., Cohen, L., Hudson, S. R., Walden, V. P., Granskog, M. A., et al. (2017). A comparison of the two Arctic atmospheric winter states observed during N-ICE2015 and SHEBA. *Journal of Geophysical Research: Atmospheres*, *122*, 5716–5737. https://doi.org/10.1002/2016JD025475

Hanson, C., Palutikof, J., & Davies, T. (2004). Objective cyclone climatologies of the North Atlantic - a comparison between the ECMWF and NCEP Reanalyses. *Climate Dynamics*, *22*(6-7), 757–769. https://doi.org/10.1007/s00382-004-0415-z

Hodges, K. I., Hoskins, B. J., Boyle, J., & Thorncroft, C. (2003). A comparison of recent re-analysis datasets using objective feature tracking: Storm tracks and tropical easterly waves. *Monthly Weather Review*, *131*(9), 2012–2037. https://doi.org/10.1175/1520-0493(2003)131%3C2012:ACORRD%3E2.0.CO;2

Kim, B.-M., Hong, J.-Y., Jun, S.-Y., Zhang, X., Kwon, H., Kim, S.-J., et al. (2017). Major cause of unprecedented Arctic warming in January 2016: Critical role of an Atlantic windstorm. *Scientific Reports*, *7*, 40051.

Kim, D., Ray, R., & Choi, M. E. (2017). Simulations of energy balance components at snow-dominated montane watershed by land surface models. *Environment and Earth Science*, *76*(9), 337. https://doi.org/10.1007/s12665-017-6655-0

Kobayashi, S., Ota, Y., Harada, Y., Ebita, A., Moriya, M., Onoda, H., et al. (2015). The JRA-55 Reanalysis: General specifications and basic characteristics. *Journal of the Meteorological Society of Japan. Ser. II*, *93*(1), 5–48. https://doi.org/10.2151/jmsj.2015-001

Laffineur, T., Claud, C., Chaboureau, J.-P., & Noer, G. (2014). Polar lows over the Nordic Seas: Improved representation in ERA-Interim compared to ERA-40 and the impact on downscaled simulations. *Monthly Weather Review*, *142*(6), 2271–2289. https://doi.org/10.1175/MWR-D-13-00171.1

Lindsay, R., Wensnahan, M., Schweiger, A., & Zhang, J. (2014). Evaluation of seven different atmospheric reanalysis products in the Arctic. *Journal of Climate*, *27*(7), 2588–2606. https://doi.org/10.1175/JCLI-D-13-00014.1

Matthes, H., Rinke, A., Miller, P. A., Kuhry, P., Dethloff, K., & Wolf, A. (2012). Sensitivity of high-resolution Arctic regional climate model projections to different implementations of land surface processes. *Climatic Change*, *111*(2), 197–214. https://doi.org/10.1007/s10584-011-0138-1

Matthes, H., Rinke, A., Zhou, X., & Dethloff, K. (2017). Uncertainties in coupled regional Arctic climate simulations associated with the used land surface model. *Journal of Geophysical Research: Atmospheres*, *122*, 7755–7771. https://doi.org/10.1002/2016JD026213

Moore, G. W. K. (2016). The December 2015 North Pole Warming Event and the Increasing Occurrence of Such Events. *Scientific Reports*, *6*, 1–11. https://doi.org/10.1038/srep39084

Neu, U., Akperov, M. G., Bellenbaum, N., Benestad, R., Blender, R., Caballero, R., et al. (2013). IMILAST: A community effort to intercompare extratropical cyclone detection and tracking algorithms. *Bulletin of the American Meteorological Society*, *94*, 529âĂŞ547(4), 529–547. https://doi.org/10.1175/BAMS-D-11-00154.1

Raible, C. C., Della Marta, P. M., Schwierz, C., Wernli, H., & Blender, R. (2008). Northern Hemisphere extratropical cyclones: A comparison of detection and tracking methods and different reanalyses. *Monthly Weather Review*, *136*(3), 880–897. https://doi.org/10.1175/2007MWR2143.1

Saha, S., Moorthi, S., Pan, H. L., Wu, X., Wang, J., Nadiga, S., et al. (2010). The NCEP Climate Forecast System Reanalysis. *Bulletin of the American Meteorological Society*, *91*(8), 1015–1058. https://doi.org/10.1175/2010BAMS3001.1

Sepp, M., & Jaagus, J. (2011). Changes in the activity and tracks of Arctic cyclones. *Climatic Change*, *105*(3-4), 577–595. https://doi.org/10.1007/s10584-010-9893-7

Serreze, M. C., & Barrett, A. P. (2008). The summer cyclone maximum over the Central Arctic Ocean. *Journal of Climate*, *21*(5), 1048–1065. https://doi.org/10.1175/2007JCLI1810.1

Simmonds, I., & Keay, K. (2009). Extraordinary September Arctic sea ice reductions and their relationships with storm behavior over 1979–2008. *Geophysical Research Letters*, *36*, L19715. https://doi.org/10.1029/2009GL039810

Simmonds, I., & Rudeva, I. (2014). A comparison of tracking methods for extreme cyclones in the Arctic basin. *Tellus A*, *66*(1). https://doi.org/10.3402/tellusa.v66.25252

Simmonds, I., Burke, C., & Keay, K. (2008). Arctic climate change as manifest in cyclone behavior. *Journal of Climate*, *21*(22), 5777–5796. https://doi.org/10.1175/2008JCLI2366.1

Sorteberg, A., & Walsh, J. E. (2008). Seasonal cyclone variability at 70°N and its impact on moisture transport into the Arctic. *Tellus A*, *60*(3), 570–586. https://doi.org/10.1111/j.1600-0870.2008.00314.x

Tilinina, N., Gulev, S. K., Rudeva, I., & Koltermann, P. (2013). Comparing cyclone life cycle characteristics and their interannual variability in different reanalyses. *Journal of Climate*, *26*(17), 6419–6438. https://doi.org/10.1175/JCLI-D-12-00777.1

Tilinina, N., Gulev, S. K., & Bromwich, D. H. (2014). New view of Arctic cyclone activity from the Arctic system reanalysis. *Geophysical Research Letters*, *41*, 1766–1772. https://doi.org/10.1002/2013GL058924

Trigo, I. F. (2006). Climatology and interannual variability of storm-tracks in the Euro-Atlantic sector: A comparison between ERA-40 and NCEP/NCAR reanalyses. *Climate Dynamics*, *26*(2-3), 127–143. https://doi.org/10.1007/s00382-005-0065-9

Ulbrich, U., Leckebusch, G. C., Grieger, J., Schuster, M., Akperov, M., Bardin, M. Y., et al. (2013). Are greenhouse gas signals of Northern Hemisphere winter extra-tropical cyclone activity dependent on the identification and tracking algorithm? *Meteorologische Zeitschrift*, *22*(1), 61–68. https://doi.org/10.1127/0941-2948/2013/0420

Vavrus, S. J. (2013). Extreme Arctic cyclones in CMIP5 historical simulations. *Geophysical Research Letters*, *40*, 6208–6212. https://doi.org/10.1002/2013GL058161

Wang, X. L., Feng, Y., Chan, R., & Isaac, V. (2016). Inter-comparison of extra-tropical cyclone activity in nine reanalysis datasets. *Atmospheric Research*, *181*, 133–153. https://doi.org/10.1016/j.atmosres.2016.06.010

Zhang, X., Walsh, J. E., Zhang, J., Bhatt, U. S., & Ikeda, M. (2004). Climatology and interannual variability of Arctic cyclone activity: 1948–2002. *Journal of Climate*, *17*(12), 2300–2317. https://doi.org/10.1175/1520-0442(2004)017%3C2300:CAIVOA%3E2.0.CO;2